FOR THE RECORD

Structures of the OmpF porin crystallized in the presence of foscholine-12

Georgia Kefala,[1,2,3] Chihoon Ahn,[1,2,3] Martin Krupa,[1,2,3] Luis Esquivies,[1,2] Innokentiy Maslennikov,[1,2] Witek Kwiatkowski,[1,2] and Senyon Choe[1,2,3]*

[1]Structural Biology Laboratory, The Salk Institute for Biological Studies, 10010 North Torrey Pines Rd., La Jolla, California 92037

[2]The Center for Structures of Membrane Proteins (CSMP), UCSF Mission Bay Campus, S414 Genentech Hall, 600 16th Street, San Francisco, California, 94107

[3]Joint Center for Biosciences, Incheon 406-840, Korea

Received 12 December 2009; Revised 10 February 2010; Accepted 12 February 2010
DOI: 10.1002/pro.369
Published online 1 March 2010 proteinscience.org

Abstract: The endogenous *Escherichia coli* porin OmpF was crystallized as an accidental by-product of our efforts to express, purify, and crystallize the *E. coli* integral membrane protein KdpD in the presence of foscholine-12 (FC12). FC12 is widely used in membrane protein studies, but no crystal structure of a protein that was both purified and crystallized with this detergent has been reported in the Protein Data Bank. Crystallization screening for KdpD yielded two different crystals of contaminating protein OmpF. Here, we report two OmpF structures, the first membrane protein crystal structures for which extraction, purification, and crystallization were done exclusively with FC12. The first structure was refined in space group P21 with cell parameters *a* = 136.7 Å, *b* = 210.5 Å, *c* = 137 Å, and β = 100.5°, and the resolution of 3.8 Å. The second structure was solved at the resolution of 4.4 Å and was refined in the P321 space group, with unit cell parameters *a* = 215.5 Å, *b* = 215.5 Å, *c* = 137.5 Å, and γ = 120°. Both crystal forms show novel crystal packing, in which the building block is a tetrahedral arrangement of four trimers. Additionally, we discuss the use of FC12 for membrane protein crystallization and structure determination, as well as the problem of the OmpF contamination for membrane proteins overexpressed in *E. coli*.

Keywords: OmpF; contamination; membrane protein; foscholine-12

Introduction

The outer membrane of gram-negative bacteria protects from harsh environmental conditions and toxic molecules such as antibiotics, proteases, and heavy metals. It is comprised of complex lipopolysccharides and a relatively small number of proteins which all form β-barrel structures. The majority of these proteins form hydrophilic pores that allow small nutrients and signaling molecules to permeate and reach the cell, and are thus called porins. In *Escherichia coli*, the major porins are the outer membrane proteins (OMP) OmpF, OmpC, and OmpE (also

Abbreviations: β-ME, β-mercaptoethanol; FC12, foscholine-12 (aka DPC, *n*-dodecylphosphocholine); M, Mistic fused protein, Misticated; NM, non-Mistic fused, non-Misticated; OG, octyl glucoside; OMP, outer membrane proteins; PCR, polymerase chain reaction; SDS–PAGE, sodium dodecyl sulfate polyacrylamide gel electrophoresis.

Grant sponsor: NIH, Protein Structure Initiative; Grant numbers: GM074929and GM74821; Grant sponsor: Korean MKE, IFEZ initiative; Korean Mest, World-Class University Program.

**Correspondence to:* Senyon Choe, Structural Biology Laboratory, The Salk Institute for Biological Studies, 10010 North Torrey Pines Rd., La Jolla, CA 92037.
E-mail: choe@salk.edu

Table I. *Structurally Characterized OmpF or OmpF Mutants*

PDB code	Resolution (Å)	Space group	Chains/AU	Crystallization detergent	Mutation/Complex	References
1HXU	3	P 3 2 1	1	octyl-POE	V18K, G131K	Ref. 6
1HXT	2.4	P 3 2 1	1	octyl-POE	R42A, R82A, D113N, E117Q, R132A	Ref. 6
1HXX	2.2	P 3 2 1	1	octyl-POE	Y106F	Ref. 6
1BT9	3	P 3 2 1	1	octyl-POE	D74A	Ref. 7
1MPF	3	P 3 2 1	1	octyl-POE	G119D	Ref. 8
2OMF	2.4	P 3 2 1	1	octyl-POE		Ref. 1
1GFM	3.5	P 3 2 1	1	octyl-POE	D113G	Ref. 9
1GFN	3.1	P 3 2 1	1	octyl-POE	DEL(109-114)	Ref. 9
1GFO	3.3	P 3 2 1	1	octyl-POE	R132P	Ref. 9
1GFP	2.7	P 3 2 1	1	octyl-POE	R42C	Ref. 9
1GFQ	2.8	P 3 2 1	1	octyl-POE	R82C	Ref. 9
2ZFG	1.6	P 3 2 1	1	octyl-POE		Ref. 10
2ZLD	3	P 63	2	octyl-POE	Complex with N-terminal segment of colicin E3	Ref. 10
1OPF	3.2	P 42	6	β-OG, (C10DAO)		Refs. 11, 12
3FYX	3.4	P 3 2 1	1	octyl-POE	K16C, chemically modified	Ref. 13
3K1B	4.4	P 3 2 1	4	foscholine-12		This work
3K19	3.8	P 21	12	foscholine-12		This work

known as PhoE). The three proteins are highly homologous, with 62% sequence identity between OmpF and OmpE, and 58% between OmpF and OmpC (mature forms). OmpF and OmpE were among the first membrane protein structures determined,[1] following the determination of the photosynthetic reaction centers of *Rhodospeudomonas viridis*[2] and *Rhodobacter sphaeroides*,[3] and the porin from *Rhodobacter capsulatus*.[4] All general porin monomers form 16-stranded β-barrels that associate in tightly packed trimers.[1,5] Their unusual stability, explained by the robustness of their structure, has been critical for their crystallization and subsequent structure determination. OmpF protein is one of the best studied membrane proteins up to now (Table I). The mature protein is comprised of 340 amino acids, and forms aqueous, voltage-gated channels that span the outer membrane and allow the diffusion of small polar molecules. Eight short β-hairpins on the periplasmic side, and eight long irregular loops (L1–L8) on the extracellular side connect the antiparallel β-strands.[1] L3 is particularly long, consisting of 33 residues and folds inside the pore, restricting its accessibility. The pore dimensions at this narrowing are about 7 × 11 Å, allowing the passage of molecules <600 Da, with slight preference for those with a positive charge.

Foscholine detergents are lipid-like zwitterionic molecules, widely used in the investigation of membrane proteins. They have the same head group as phospholipids, but a single hydrophobic tail, which leads to the formation of micelles rather than bilayers. This is the main reason why these detergents are extremely efficient in *E. coli* membrane solubilization,[14,15] and foscholine-12 (FC12) with 12 methylene hydrophobic groups is one of the most effective membrane solubilization agents. FC12 has also been extremely useful and popular in NMR studies of membrane proteins aiming to obtain high-resolution spectra in mixed micelles,[16] and has been shown to play a crucial role in refolding misfolded membrane proteins.[17] When it comes to membrane protein crystallization, octyl glucoside (OG) remains the most extensively used detergent, with lauryldimethylamine oxide (LDAO) following closely.[16] Although crystallization of a membrane protein in the presence of FC12 has been reported,[16] there is no crystal structure of a protein that would be both purified and crystallized with FC12. Therefore, it is believed that FC12 is of limited use for membrane protein crystallography. However, a recent analysis of 43 eukaryotic membrane proteins expressed in *Saccharomyces cerevisiae*, showed that 70% of the well-expressed membrane proteins were stable, targeted to the correct organelle, and monodisperse in either FC12 or *n*-dodecyl-β-D-maltoside.[18] Refuting the negative opinion about the use of FC12 in membrane protein crystallography we present here two different crystal forms of the structure of the OmpF porin, for which the protein was exclusively treated with FC12 throughout the extraction, purification, and crystallization processes. We also report two new modes of crystal packing of OmpF in the presence of FC12.

Results and Discussion

OmpF identification and structure solution

In the process of crystallization of the *E. coli* histidine kinase receptor KdpD, we obtained small crystals (about 50 μm) of different morphology [Fig. 1(A,B)] that diffracted to about 10–15 Å. Crystals have been further optimized to diffract X-rays to 3.5–5 Å. Our efforts to solve the structure by molecular replacement using the crystal structure of the

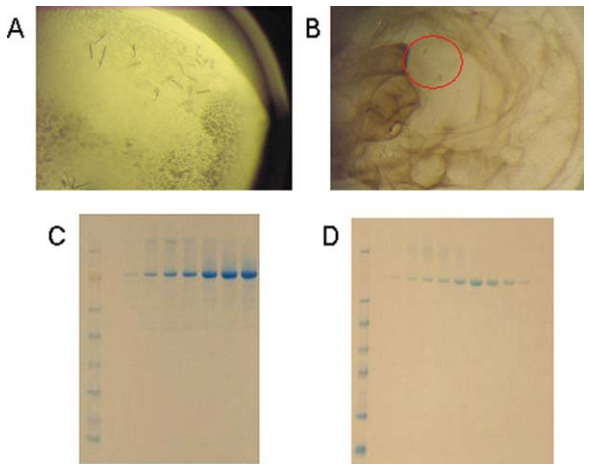

Figure 1. Purification and crystallization of KdpD protein. (A) KdpD-M and (B) KdpD-NM crystals. Both were proved to be OmpF. (C) KdpD-M and (D) KdpD-NM fractions after size exclusion chromatography, used for crystallization trials.

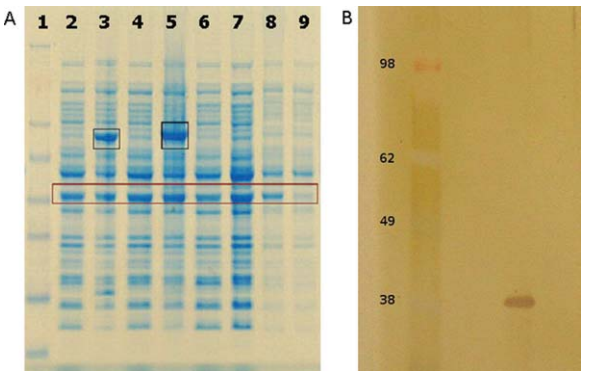

Figure 2. (A) OmpF expression in BL21(DE3) cells. NuPAGE (4–12%) Bis-Tris SDS gel. Lane 1: See blue plus 2 protein standard (Invitrogen). Lanes 2 and 4: Cells before induction of recombinant protein expression. Lanes 3 and 5: Cells after induction of recombinant membrane protein expression, and after induction of the same membrane protein in fusion with Mistic, respectively. Lane 6: Control BL21(DE3) cells grown in parallel with the transformed and induced cells. Sample taken at the same time point as samples in lanes 2 and 4. Lane 7: Control BL21(DE3) cells grown in parallel with the transformed and induced cells. Sample taken at the same time point as samples in lanes 3 and 5. Lane 8: Control BL21(DE3) whole cell lysate. Lane 9: Control BL21(DE3) supernatant after centrifugation for 1 h at 100,000*g*. In black boxes are the expressed target proteins. In the brown box the highly expressed OmpF porin is highlighted. (B) SDS–PAGE of OmpF, silver stained. The molecular weigh of the OmpF monomer is about 37 kDa.

N-terminal region (19–243) of KdpD from *Pseudomonas syringae* pv. tomato str. DC3000 [Protein Data Bank (PDB) code: 2R8R] were futile. Although the protein preparation looked very clean on sodium dodecyl sulfate polyacrylamide gel electrophoresis (SDS–PAGE) [Fig. 1(C,D)], we suspected contamination from the endogenous *E. coli* porin OmpF since this protein is known to express at high levels during overexpression of membrane proteins in *E. coli*,[19] including histidine kinase receptors [Fig. 2(A) and Ref. (20)]. N-terminal amino acid sequencing had previously confirmed that the highly expressed protein is mature OmpF (N terminus at amino acid 29). The N-terminal sequencing reading was long enough (12 residues: AEIYNKDGNKVD) to ensure that the protein is OmpF and not some other closely related Omp protein. To identify the crystallized protein, we carefully washed the crystals and ran a silver stain gel that showed a protein of about ~38 kDa [Fig. 2(B)], compatible with the expected OmpF monomer size. Molecular replacement using the protein sequence for the *E. coli* BL21(DE3) strain OmpF (Uniprot C6EI53) [which is identical to the sequence for the *E. coli* K12 strain OmpF (Uniprot P02931)] did indeed give a clear solution, with MR scores 23.13 for the P21 crystal form, and 18.91 for the P321 crystal form.

Crystal packing of OmpF prepared in FC12

OmpF crystallized in two different space groups, P21 and P321, with crystal packings not observed previously. The most common packing observed for

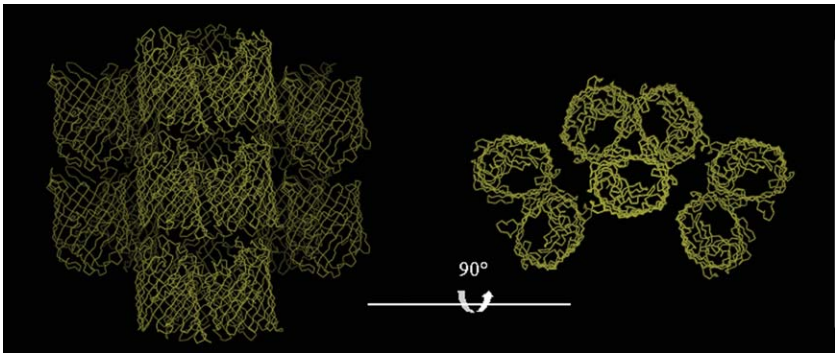

Figure 3. Previously reported crystal packing in the common P321 crystal form. Linear stacking of OmpF trimers, with neighboring columns running in opposite directions, and 90° rotation. PDB code: 2OMF (1).

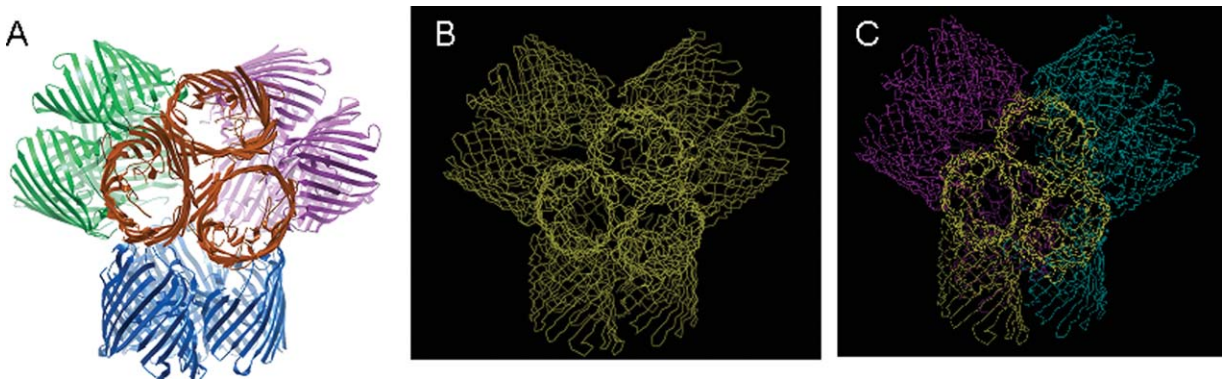

Figure 4. The tetrahedron arrangement: (A) Four trimers (shown here in different colors) form a tetrahedron. (B) The tetrahedron in the P21 structure reported here (PDB code: 3K19). (C) The tetrahedron in the P321 structure reported here (PDB code: 3K1B). In (B) and (C) the contents of the asymmetric unit are represented in different colors. In (C), trimers forming one arm of the tetrahedron and one monomer of the arm of a neighboring trimer form the asymmetric unit.

14 of 15 previously observed OmpF structures is the linear stacking of OmpF trimers, with neighboring columns running in opposite directions. This arrangement is observed in all 13 P321 space groups reported so far, and in the P63 space group in the complex of OmpF with the N-terminal segment of colicin E3 (Table I, Fig. 3). In contrast, the building block of the crystal packing observed in this study is a tetrahedral arrangement of OmpF trimers for both space groups (Fig. 4). The tetrahedral arrangement was observed in space group P42 previously reported.[11,12] In that case crystals were grown from solutions containing 0.9% β-OG and 0.09% C8E6-11. The asymmetric unit contains two trimers, and two pairs of trimers from adjacent asymmetric units form a tetrahedron. In our structures the same tetrahedron is the building block for both packings: in the P21 crystal the tetrahedron is formed by the four tetrahedrally arranged trimers of the asymmetric unit, while in the P321 crystal the asymmetric unit consists of a trimer and a monomer, and three adjacent asymmetric units assemble into one tetrahedron identical to the one observed in the P21 space group. Thus, the same tetrahedron, arranged so that the rough end of each monomer is oriented towards the center of the tetrahedron, is the building unit of all three crystal packings mentioned above (P42, P21, and P321). Remarkably, each tetrahedron forms four contacts in the crystal lattices of these three space groups. There are two possible types of contacts observed so far: corner-to-corner contact, made between the smooth ends of adjacent tetrahedra [Fig. 5(A)] and detergent mediated corner-to-center contact with the smooth end of one tetrahedron oriented towards the center of the neighboring one [Fig. 5(B)]. In the previously reported P42 crystal form,[11] each tetrahedron forms identical crystallographically related lattice contacts at its four corners [Fig. 6(A)]. In the structures we report here, each tetrahedron forms two corner-to-corner and two corner-to-center lattice contacts in the P21 crystal form [Fig. 6(B)], or three corner-to-corner

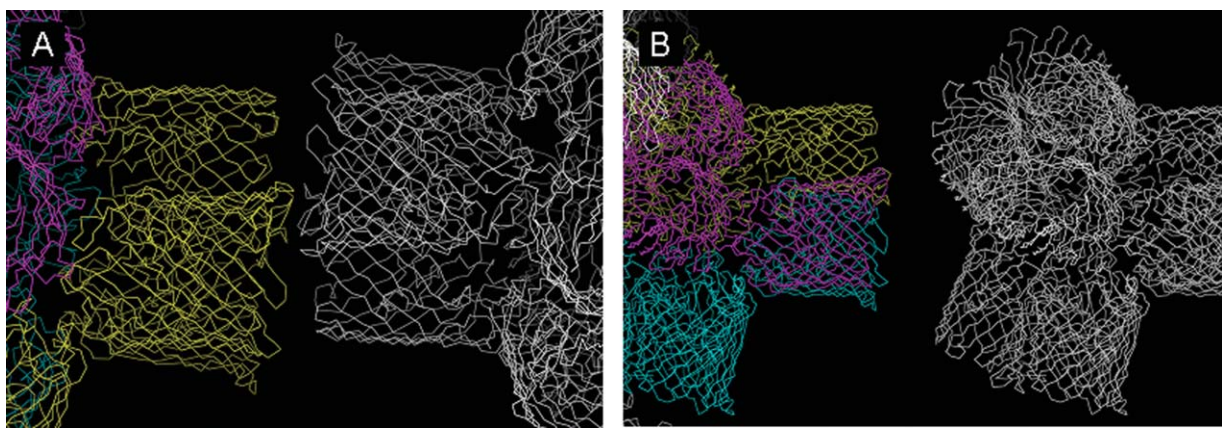

Figure 5. The two types of contacts between tetrahedra in the crystal packings (P21 and P321) reported here. (A) Corner-to-corner contact involving the edges of two adjacent tetrahedra. (B) Corner-to-center contact with the smooth end of one tetrahedron oriented toward the center of the neighboring one, where the rough ends of all four trimers are clustered.

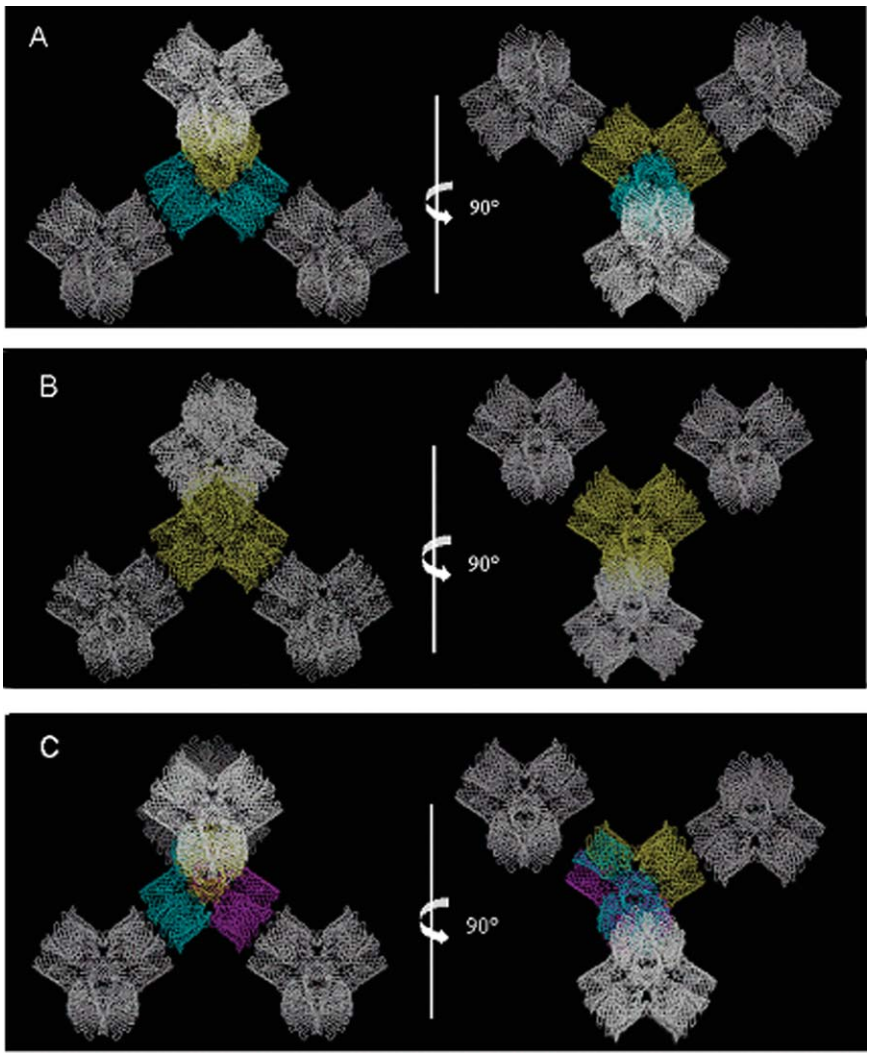

Figure 6. Tetrahedron contacts. (A) The P42 crystal form (PDB code: 11PF) (11) and 90° rotation. (B) The P21 crystal form (PDB code: 3K19) and 90° rotation. (C) The P321 crystal form (PDB code: 3K1B) and 90° rotation. The asymmetric unit contents are shown in different colors. In (A), the asymmetric unit content is a pair of trimers, in (B) it is a tetrahedron (two pairs of trimers), and in (C) it is one trimer forming one arm of the tetrahedral unit plus one monomer of the neighboring arm of the tetrahedron. Neighboring tetrahedra are shown in white.

and one corner-to-center contacts in the P321 crystal form [Fig. 6(C)], resulting in dramatically different packing arrangements. This difference in crystal contacts must be due to the effects of crystallization conditions, such as ionic strength and pH, on detergent-induced surface properties.

In general, the impact of the type of detergent on crystal packing can be very powerful. The widely used *N*-octyl-polyoxyethylene (octyl-POE) (Table I and Refs. 1, 6, 13), results in linear stacking of OmpF trimers, whereas β-OG and FC12 give rise to tetrahedral arrangements of trimers, which shows that FC12 can work successfully in membrane protein crystallization, just like the detergent β-OG. To our knowledge, the reported structures are the first membrane protein structures for which all steps of extraction, purification and crystallization were performed in the presence of FC12, a very potent detergent in membrane protein studies, especially when an *E. coli* expression system is used. According to the Membrane PDB,[16] two membrane proteins have been crystallized in the presence of FC12, but one of them was extracted and purified in a different detergent[21,22] and the second was crystallized in a mixture of two detergents.[23] In particular, the zinc transporter YiiP (PDB code: 2QFI) was crystallized in the presence of FC12 in the reservoir solution,[21] but it was extracted and purified in the presence of DDM,[22] so DDM was present in the crystallization sample as well. In the second case, the rat monoamine oxidase A was extracted and purified in FC12, but 0.8% (w/v) dimethyldecylphosphine oxide was also present during crystallization, in addition to 0.05% (w/v) FC12.[23] There is one reported case of a membrane protein being

extracted, purified, and crystallized in another foscholine detergent, FC14, the *E. coli* mechanoselective channel McsC.[24,25]

OmpF overexpression during recombinant membrane protein expression in E. coli

Recenly, the first crystal structure of a human membrane protein expressed in *E. coli*[26,27] has renewed interest in *E. coli*-based expression of mammalian membrane proteins.[28,29] OmpF contamination is a major issue that needs to be seriously considered. We have observed and verified by N-terminal sequencing that OmpF overexpresses abundantly during recombinant *E. coli* expression of different families of membrane proteins, including human membrane proteins. OmpF expression does not seem to be linked to the induction of particular recombinant protein overexpression: we have grown BL21(DE3) cells, as a control, in parallel with cultures expressing recombinant membrane proteins, and the amount of expressed OmpF is very comparable between the control cells and the cells expressing the recombinant proteins [Fig. 2(a)]. Moreover, we see similar OmpF expression patterns for both Misticated and non-Misticated proteins,[20] so fusion with Mistic does not seem to affect OmpF expression. Small contamination by OmpF in a membrane protein preparation has been reported before in the case of the vitamin B12 transporter BtuB.[30] OmpF overexpression is not surprising as porins are one of the most abundant protein families in bacteria. Depending on the bacterial species and the growth conditions, gram-negative bacteria typically have about 10^5 copies of general porins per cell.[31] The presence of OmpF is, however, a cause for concern when purifying membrane proteins for structural studies. As we report here, OmpF crystallization can occur opportunistically even from trace amounts in a solution of target protein concentrations of 10–15 mg/mL, due to its unusual stability. Due to the minimal amount of OmpF in the solution, crystallization was slow and it took 4–6 weeks for the crystals to grow, which prompted us to check the identity of the crystallized protein by silver stain SDS–PAGE [Fig. 2(B)]. The choice of cell lysis method doesn't impact on OmpF contamination significantly, as evidenced by comparable levels of contamination either using a microfluidizer or a sonication protocol. The solubilization stage, however, is critical for minimizing the contamination risk. Special care is needed in cases where the only detergent that can efficiently extract the protein of interest is also a good extractor for porins or other endogenous *E. coli* membrane proteins, as was the case for KdpD.

Given that OmpF is not rich in histidine residues (one in 362 residues, one in 340 for the mature protein), and that the molecular weight of the OmpF trimer is about 110 kDa versus 234 kDa of the KdpD-M dimer and 204 kDa of the KdpD-NM dimer, it is striking that OmpF is still present (although in amounts not detected by SDS–PAGE) in our samples after the immobilized metal ion affinity chromatography and the size exclusion purification steps. To avoid OmpF contamination in the future, we have incorporated in our routine purification protocol an ion exchange purification step. This helps ensuring good separation in cases where the pI of the protein of interest is at least 2 pH units different from the OmpF pI (theoretical pI: 4.6).

The expression of OMP proteins is tightly regulated so that the total porin amount remains constant. The OmpF/OmpC ratio is dependent on factors such as osmolarity and pH of the growth medium, antibiotic concentration, cell density, and bacterial strain.[32] In media of high osmolarity, OmpC is expressed at the expense of OmpF. The smaller pore of OmpC slows down the diffusion rate of small molecules and this might be beneficial in the bacterium's natural environment, the intestine, where nutrient concentration, but also the concentration of toxic molecules such as bile salts, is relatively high. In conditions where nutrient concentration is low, OmpF becomes the major porin.[33] In Gram-negative bacteria the development of resistance to β-lactam antibiotics depends, in addition to the production of lactamase enzymes, on down-regulation of porin expression, or porin functional modification through mutation.[34–36] Nonetheless, it has been reported that under antibiotic stress, OmpF was preferentially lost in *E. coli* K-12, but OmpC was overproduced, and the strain showed resistance to only some β-lactams.[37] In the light of this finding, increasing the antibiotic concentration during recombinant protein expression when ampicillin/carbenicillin resistance is used, might help with reducing the amount of expressed OmpF, but the total porin amount is likely to remain the same.

In this study we used the *E. coli* strain BL21(DE3), one of the most commonly used strains for recombinant protein expression. Analysis of the outer membrane fraction of different *E. coli* strains has previously shown that OmpF expression is particularly elevated in BL21(DE3), compared to strains HB101, JM101, MC4100, XL1-Blue, and W3110.[38] It has been reported that the difference in OmpF expression between the *E. coli* BL21(DE3) and K12 strain might be explained by two mutations at positions –18 and –363 in the ompF promoter and its upstream region. Position –363 is within the OmpR binding site,[39] so the mutation seems to affect OmpR binding, and thus the repression of ompF expression. We have prepared a BL21(DE3) ompF knock-out strain for protein expression for a future comparison study. Nonetheless, caution must be exercised because it has been reported that in *E. coli* BL21(DE3) ompF knock-outs, OmpF expression is abolished but the expression of OmpC is increased.[38]

Table II. *Refinement and Model Statistics for OmpF*

	3K1B	3K19
Space group	P 3 2 1	P 21
Cell dimensions	$a = 215.5$ Å, $b = 215.5$ Å, $c = 137.5$ Å, $\gamma = 120°$	$a = 136.7$ Å, $b = 210.5$ Å, $c = 137$ Å, $\beta = 100.5°$
Resolution limits (Å)	49.23-4.39 (4.5-4.39)	49.58-3.79 (3.89-3.79)
Completeness (%)	99 (98.14)	98.9 (87.5)
Data cutoff [F/s(F)]	0.0	0.0
Number of reflections	23,572	74,966
Working set	22,361	71,179
Test set	1211	3787
R_{cryst} (%)	26.4 (28)	28 (34.4)
R_{free} (%)	32.9 (33.5)	28.8 (32.4)
Number of atoms	10,500	31,492
R.m.s. deviations		
Bonds (Å)	0.027	0.004
Angles (°)	2.86	0.650
Average B factor for protein (Å^2)	126.423	78.133
Ramachandran plot		
Most favoured (%)	73.3	89.74
Additionally allowed (%)	15.9	6.71

Values in parenthesis indicate the highest resolution shell.

Materials and Methods

All chemicals were purchased from Sigma, unless otherwise noted. NuPAGE gels and the SeeBlue +2 protein standard were from Invitrogen. Detergents were purchased from Anatrace.

Cloning and expression

The kdpD gene from *E. coli* K12 MG1655 was amplified and Gateway (Invitrogen) adapted by performing two successive rounds of polymerase chain reaction (PCR). In the first round, gene-specific primers and a single cell *E. coli* colony as template were used. After PCR purification (Qiagen), the product of the first PCR served as the template for the second PCR, and a pair of generic primers was used to introduce the attB sites required for Gateway cloning and an N-terminal thrombin cleavage site. The final PCR product was gel-purified (Qiagen), and used to set up a BP reaction with the pENTR207 vector, following the manufacturer's instructions (Invitrogen). Two different expression constructs were prepared, with or without the membrane-targeting protein Mistic[40] fused to the N-terminus of the protein. Both vectors are pET derived, Gateway adapted, and add an N-terminal histidine tag to the expressed proteins. The recombinant plasmids were used to transform *E. coli* BL21(DE3) cells (Invitrogen). Cells from an overnight 5 mL culture were inoculated in 6 L of Terrific Broth medium and grown at 37°C to an OD 600 nm^{-1}. The temperature was then lowered to 18°C and protein production was induced by the addition of 0.5 m*M* β-D-thiogalactopyranoside, followed by overnight (about 16 h) incubation. Cells were lysed either by three sonication cycles 1 min each, using 1 s pulses, on ice, or by three microfluidizer cycles (M-110L Microfluidizer Processor from Microfluidics) at 18,000 psi.

The membrane isolation protocol has been previously reported.[20] In brief, it consists of an initial high-speed centrifugation to remove soluble proteases as soon as possible after cell disruption, followed by a soft spin to remove inclusion bodies, and after overnight solubilization in a high salt buffer to remove electrostatically bound proteins, we pellet the membrane fraction by a final high-speed centrifugation.

Protein purification

KdpD was extracted from the membrane with 20 m*M* FC12 for 2 h at 4°C in a buffer containing 20 m*M* Tris pH 8, 200 m*M* NaCl, 1 m*M* $MgCl_2$, 5 m*M* β-mercaptoethanol (β-ME), 10% v/v glycerol, and one Complete Mini EDTA-free protease-inhibitor cocktail tablet (Roche) per 20 mL. The solubilized membrane protein fraction was separated by centrifugation for 60 min at 100,000*g*. The supernatant was filtered through a 0.22 μm membrane and was incubated with 5 mL Ni-NTA (Qiagen) beads for 40 min at 4°C. The beads were then packed into a column, and the flow through was collected and reloaded to the column. To remove unbound proteins, the column was washed with 50 mL of 20 m*M* Tris pH 8.0, 200 m*M* NaCl, 20 m*M* imidazole, 5% (v/v) glycerol, 2 m*M* β-ME, 5 m*M* FC12. The protein was eluted in three column volumes with 20 m*M* Tris pH 8.0, 200 m*M* NaCl, 300 m*M* imidazole, 5% (v/v) glycerol, 2 m*M* β-ME, and 5 m*M* FC12. After SDS–PAGE, the KdpD containing fractions were pooled and concentrated using a 100 kDa molecular weight cut-off concentrator (Vivaspin) and subsequently purified by gel filtration (Superdex 200, 16/60; GE Healthcare) in a buffer containing 20 m*M* Tris pH 8.0, 200 m*M* NaCl, 5%(v/v) glycerol, 1 m*M* dithiothreitol, and 2 m*M* FC12. The peak fractions

were analyzed by SDS–PAGE [Fig. 1(C,D)], pooled and concentrated. The purity of the protein was estimated by SDS–PAGE and its oligomeric state was probed by static light scattering and refractive index.

Crystallization, data collection and structure determination

The protein was concentrated to 10–15 mg/mL and initial crystallization trials were performed using our in-house Honeybee crystallization robot (Genomic Solutions). Crystals were obtained at 20°C after 4–6 weeks in 0.4 *M* NaH_2PO_4/1.6 *M* K_2HPO_4, 0.1 *M* Imidazole pH 8, 0.2 *M* NaCl (Emerald Biosciences Wizard I condition 20) for the non-Misticated KdpD (KdpD-NM) sample, and in 0.1 *M* acetate pH 4.5, 0.8 *M* NaH_2PO_4/1.2 *M* K_2HPO_4 (Emerald Biosciences Wizard II condition 35), later optimized to 0.1 *M* Acetate pH 3.9, 0.48 *M* NaH_2PO_4/0.72 *M* KH_2PO_4, for the Misticated KdpD (KdpD-M) sample. Diffraction data were collected at the Advanced Light Source (Berkeley, CA) on beamline 8.2.1 using an ADSC Q315r 3 × 3 CCD detector at -100°C. Data were processed and scaled with the HKL2000 package.[41] The crystal harvested from the KdpD-NM crystallization drop diffracted X-rays to 3.8 Å resolution and belongs to space group P21 with cell parameters a = 136.7 Å, b = 210.5 Å, c = 137 Å, and β = 100.5°. The crystal harvested from the KdpD-M crystallization drop diffracted to 4.4 Å resolution and belongs to the P321 space group, with unit cell parameters a = 215.5 Å, b = 215.5 Å, c = 137.5 Å, and γ = 120°. Our various attempts to solve the structure by molecular replacement using the structure of the N-terminal region (residues 19–243) of *P. syringae* pv. tomato str. DC3000 KdpD (PDB code 2R8R) as a search model, with the program MOLREP[42] and the molecular replacement automatic suit BALBES,[43] failed. Surprisingly, however, molecular replacement using the amino acid sequence of OmpF with BALBES did give a clear solution, using the OmpF structure 1HXX[6] as the search model. The MR scores were 23.13 for the P21 crystal form, and 18.91 for the P321 crystal form. The structures were refined with REFMAC5[44] and model building was performed using COOT.[45] The structures were refined to *R*cryst and *R*free factors of 26.4% and 32.9% for the P321 structure, and 28% and 28.8% for theP21 structure. Data processing and refinement statistics are summarized in Table II. Atomic coordinates and structure factors have been deposited in the RCSB PDB, under the accession codes 3K1B and 3K19. Figures were prepared using the programs PyMol[46] and O.[47]

Concluding Remarks

Two structures of the OmpF porin with different packing properties were solved. These are the first structures of membrane proteins exclusively treated with FC12, showing that FC12 proves a useful detergent for crystallization screening.

OmpF contamination can be a potentially systematic problem in *E. coli*-based membrane protein expression. Approaches to minimize the problem might include careful monitoring of growth conditions, selection of a low porin-expressing strain, and sucrose gradient centrifugation to separate inner and outer membranes. After expression, an optimized two-step extraction protocol might be applied, when the target protein can be extracted by a small number of specific detergents.

Acknowledgment

We would like to thank the staff at the Advanced Light Source (Berkeley) for providing beam time.

References

1. Cowan SW, Schirmer T, Rummel G, Steiert M, Ghosh R, Pauptit RA, Jansonius JN, Rosenbusch JP (1992) Crystal structures explain functional properties of two *Escherichia coli* porins. Nature 358:727–733.
2. Deisenhofer J, Epp O, Miki K, Huber R, Michel H (1985) Structure of the protein subunits in the photosynthetic reaction centre of *Rhodospeudomonas viridis* at 3 Å resolution. Nature 318:618–624.
3. Yeates TO, Komiya H, Rees DC, Allen JP, Feher G (1987) Structure of the reaction center from *Rhodobacter sphaeroides* R-26: membrane-protein interactions. Proc Natl Acad Sci USA 84:6438–6442.
4. Weiss MS, Schulz GE (1992) Structure of porin refined at 1.8 Å resolution. J Mol Biol 227:493–509.
5. Baslé A, Rummel G, Storici P, Rosenbusch J, Schirmer T (2006) Crystal structure of osmoporin OmpC from *E. coli* at 2.0 Å. J Mol Biol 362:933–942.
6. Phale PS, Philippsen A, Widmer C, Phale VP, Rosenbusch JP, Schirmer T (2001) Role of charged residues at the OmpF porin channel constriction probed by mutagenesis and simulation. Biochemistry 40:6319–6325.
7. Phale PS, Philippsen A, Kiefhaber T, Koebnik R, Phale VP, Schirmer T, Rosenbusch JP (1998) Stability of trimeric OmpF porin: the contributions of the latching loop L2. Biochemistry 37:15663–15670.
8. Jeanteur D, Schirmer T, Fourel D, Simonet V, Rummel G, Widmer C, Rosenbusch JP, Pattus F, Pagès, JM (1994) Structural and functional alterations of a colicin-resistant mutant of OmpF porin from *Escherichia coli*. Proc Natl Acad Sci USA 91:10675–10679.
9. Lou KL, Saint N, Prilipov A, Rummel G, Benson SA, Rosenbusch JP, Schirmer T (1996) Structural and functional characterization of OmpF porin mutants selected for larger pore size. J Biol Chem 271:20669–20675.
10. Yamashita E, Zhalnina MV, Zakharov SD, Sharma O, Cramer WA (2008) Crystal structures of the OmpF porin: function in a colicin translocon. EMBO J 27: 2171–2180.
11. Cowan SW, Garavito RM, Jansonius JN, Jenkins JA, Karlsson R, König N, Pai EF, Pauptit RA, Rizkallah PJ, Rosenbusch JP, Rummel G, Schirmer T (1995) The structure of OmpF porin in a tetragonal crystal form. Structure 3:1041–1050.
12. Pebay-Peyroula E, Garavito RM, Rosenbusch JP, Zulauf M, Timmins PA (1995) Detergent structure in

tetragonal crystals of OmpF porin. Structure 3:1051–1059.
13. Reitz S, Cebi M, Reiss P, Studnik G, Linne U, Koert U, Essen, LO (2009) On the function and structure of synthetically modified porins. Angew Chem Int Ed Engl 48:4853–4857.
14. Maslennikov I, Kefala G, Johnson C, Riek R, Choe S, Kwiatkowski W (2007) NMR spectroscopic and analytical ultracentrifuge analysis of membrane protein detergent complexes. BMC Struct Biol 7:74.
15. Maslennikov I, Krupa M, Dickson C, Esquivies L, Blain K, Kefala G, Choe S, Kwiatkowski W (2009) Characterization of protein detergent complexes by NMR, light scattering, and analytical ultracentrifugation. J Struct Funct Genomics 10:25–35.
16. Raman P, Cherezov V, Caffrey M (2006) The membrane Protein Data Bank. Cell Mol Life Sci 63:36–51.
17. Gorzelle BM, Nagy JK, Oxenoid K, Lonzer WL, Cafiso DS, Sanders CR (1999) Reconstitutive refolding of diacylglycerol kinase, an integral membrane protein. Biochemistry 38:16373–16382.
18. Newstead S, Kim H, von Heijne G, Iwata S, Drew D (2007) High-throughput fluorescent-based optimization of eukaryotic membrane protein overexpression and purification in *Saccharomyces cerevisiae*. Proc Natl Acad Sci USA 104:13936–13941.
19. Wagner S, Baars L, Ytterberg AJ, Klussmeier A, Wagner CS, Nord O, Nygren PA, van Wijk KJ, de Gier JW (2007) Consequences of membrane protein overexpression in *Escherichia coli*. Mol Cell Proteomics 6: 1527–1550.
20. Kefala G, Kwiatkowski W, Esquivies L, Maslennikov I, Choe S (2007) Application of Mistic to improving the expression and membrane integration of histidine kinase receptors from *Escherichia coli*. J Struct Funct Genomics 8:167–172.
21. Lu M, Fu D (2007) Structure of the zinc transporter YiiP. Science 317:1746–1748.
22. Chao Y, Fu D (2004) Thermodynamic studies of the mechanism of metal binding to the *Escherichia coli* zinc transporter YiiP. J Biol Chem 279:17173–17180.
23. Ma J, Yoshimura M, Yamashita E, Nakagawa A, Ito A, Tsukihara T (2004) Structure of rat monoamine oxidase A and its specific recognitions for substrates and inhibitors. J Mol Biol 338:103–114.
24. Bass RB, Strop P, Barclay M, Rees DC (2002) Crystal structure of *Escherichia coli* MscS, a voltage-modulated and mechanosensitive channel. Science 298:1582–1587.
25. Wang W, Black SS, Edwards MD, Miller S, Morrison EL, Bartlett W, Dong C, Naismith JH, Booth IR (2008) The structure of an open form of an *E. coli* mechanosensitive channel at 3.45 Å resolution. Science 321:1179–1183.
26. Xu S, McKeever BM, Wisniewski D, Miller DK, Spencer RH, Chu L, Ujjainwalla F, Yamin TT, Evans J F, Becker JW, Ferguson AD (2007) Expression, purification and crystallization of human 5-lipoxygenase-activating protein with leukotriene-biosynthesis inhibitors. Acta Crystallogr F Struct Biol Cryst Commun 63:1054–1057.
27. Ferguson AD, McKeever BM, Xu S, Wisniewski D, Miller DK, Yamin TT, Spencer RH, Chu L, Ujjainwalla F, Cunningham BR, Evans JF, Becker, JW (2007) Crystal structure of inhibitor-bound human 5-lipoxygenase-activating protein. Science 317:510–512.
28. Link AJ, Skretas G, Strauch EM, Chari NS, Georgiou G (2008) Efficient production of membrane-integrated and detergent-soluble G protein-coupled receptors in *Escherichia coli*. Protein Sci 17:1857–1863.
29. Massey-Gendel E, Zhao A, Boulting G, Kim HY, Balamotis MA, Seligman LM, Nakamoto RK, Bowie JU (2009) Genetic selection system for improving recombinant membrane protein expression in *E. coli*. Protein Sci 18:372–383.
30. Zakharov SD, Cramer WA (2004) On the mechanism and pathway of colicin import across the *E. coli* outer membrane. Front Biosci 9:1311–1317.
31. Luckey M, Bundles and barrels. In: (2008) Membrane structural biology: with biochemical and biophysical foundations. Cambridge University Press, New York, pp 102–126.
32. Alphen WV, Lugtenberg B (1977) Influence of osmolarity of the growth medium on the outer membrane protein pattern of *Escherichia coli*. J Bacteriol 131:623–630.
33. Pratt LA, Hsing W, Gibson KE, Silhavy TJ (1996) From acids to osmZ: multiple factors influence synthesis of the OmpF and OmpC porins in *Escherichia coli*. Mol Microbiol 20:911–917.
34. Pagès JM, Role of bacterial porins in antibiotic susceptibility of Gram-negative bacteria. In: Benz R, Ed. (2004) Bacterial and eukaryotic porins. Wiley-VCH: Chichester, pp 41–59.
35. Nikaido H, Normark S (1987) Sensitivity of *Escherichia coli* to various beta-lactams is determined by the interplay of outer membrane permeability and degradation by periplasmic beta-lactamases: a quantitative predictive treatment. Mol Microbiol 1:29–36.
36. Nikaido H (2003) Molecular basis of bacterial outer membrane permeability revisited. Microbiol Mol Biol Rev 67:593–656.
37. Harder KJ, Nikaido H, Matsuhashi M (1981) Mutants of *Escherichia coli* that are resistant to certain beta-lactam compounds lack the ompF porin. Antimicrob Agents Chemother 20:549–552.
38. Jeong KJ, Lee SY (2002) Excretion of human beta-endorphin into culture medium by using outer membrane protein F as a fusion partner in recombinant *Escherichia coli*. Appl Environ Microbiol 68:4979–4985.
39. Huang KJ, Schieberl JL, Igo MM (1994) A distant upstream site involved in the negative regulation of the *Escherichia coli* ompF gene. J Bacteriol 176: 1309–1315.
40. Roosild TP, Greenwald J, Vega M, Castronovo S, Riek R, Choe S (2005) NMR structure of Mistic, a membrane-integrating protein for membrane protein expression. Science 307:1317–1321.
41. Otwinosky Z, Minor W (1997) Processing of X-ray diffraction data collected in oscillation mode. Methods Enzymol 276:307–326.
42. Vagin A, Teplyakov A (1997) MOLREP: an automated program for molecular replacement. J Appl Crystallogr 30:1022–1025.
43. Long F, Vagin A, Young P, Murshudov GN (2008) BALBES: a molecular replacement pipeline. Acta Crystallogr D Biol Crystallogr 64:125–132.
44. Murshudov GN, Vagin AA, Dodson EJ (1997) Refinement of macromolecular structures by the maximum-likelihood method. Acta Crystallogr D Biol Crystallogr 53:240–255.
45. Emsley P, Cowtan K (2004) Coot: model-building tools for molecular graphics. Acta Crystallogr D Biol Crystallogr 60:2126–2132.
46. DeLano WL (2002) The PymoL Molecular Graphics System. DeLano Scientific, San Carlos, CA: DeLano Scientific.
47. Jones TA, Zou JY, Cowan SW, Kjeldgaard M (1991) Improved methods for building protein models in electron density maps and the location of errors in these models. Acta Crystallogr A Found Crystallogr 47: 110–119.